Turbulent impurity transport in DIII-D plasmas with on-axis electron heating

T. Odstrcil[1], N.T. Howard[1], F. Sciortino[1], P. Rodriguez-Fernandez[1], K.E. Thome[2], E. Hollmann[3]

[1]*MIT Plasma Science and Fusion Center, Cambridge, Massachusetts 02139, USA*

[2]*General Atomics, San Diego, CA 92121, USA*

[3]*University of California, San Diego, CA 92521, USA*

Introduction

Impurity accumulation in the plasma core presents a serious threat to the performance of fusion reactors due to fuel dilution and excessive radiative cooling. On-axis electron cyclotron resonance heating (ECRH) is often considered the most effective tool to control impurity density. However, the mechanisms by which on-axis heating stimulates impurity removal are not clear. Heating is known to modify both neoclassical and anomalous contributions to impurity transport through changes in the background profiles as well as the core MHD activity. In this paper we present dedicated experiments on the DIII-D tokamak to better understand these effects and maximize beneficial effect of core ECRH.

Setup of Impurity Transport Experiment

A set of a neutral beam injection (NBI) and ELMy H-mode discharges have been produced on DIII-D to study transport of medium and high-Z impurities - Al and W. Both species are injected by a recently installed laser blow-off (LBO) system, ablating $\sim 10^{17}$ to $2\cdot 10^{18}$ particles of W or Al per injection. The impurity source rate is determined from a visible camera with 5 kHz frame-rate observing the LBO port. Propagation of the impurity in the plasma core was observed by two SXR cameras with 32 lines of sight (LOS) each, placed symmetrically above and below the outboard midplane. These cameras are equipped with a filter wheel [3], enabling switching between 12.7 μm (efficiency $\varepsilon > 10\%$ for photons energies E_γ above 1.0 keV) and 127 μm ($\varepsilon > 10\%$ for $E_\gamma > 2.1$ keV) thick Be filters.

All discharges were performed in the same plasma shape in a lower single null configuration, with elongation $\kappa = 1.86$, lower triangularity $\delta_l = 0.6$ and upper $\delta_u = 0.3$. A moderate value of edge safety factor $q_{95} = 5.6$ at $B_T = -1.96$ T and $I_p = 0.9$ MA, was required to avoid MHD activity (including a sawteeth) and B_T was constrained by the requirements of on-axis ECRH The current flattop was split into three phases with different heating mixes. Radial profiles of T_i, T_e, n_e and inverse scale lengths of these profiles are displayed in Fig. 1. The first phase was heated with 2.9 MW of ECRH at $\rho_t = 0.25$ ($\rho_t = 0.4$ for off-axis cases) and 2 MW of NBI power between 1.4 and 2.5 s with impurity injection at 2.0 s. The high fraction of electron heating and low electron density $\langle n_e \rangle = 4.9\cdot 10^{19}\,\mathrm{m}^{-3}$ caused decoupling of electron and ions, resulting in $T_e/T_i \sim 1.6$ in plasma center, significantly peaked T_e and flat T_i profiles ($R/L_{T_e} \sim 2\cdot R/L_{T_i}$). In the second phase from 2.5 to 4.0 s, the ECRH power is reduced to 1.8 MW and the NBI power is increased to 3.4 MW with an LBO injection at 3.0 s, with a 1.0 s window before a transition to the next heating step. In these conditions, the core T_i and T_e were approximately

equal with a slightly more peaked T_e due to central ECRH. In the last phase between 4.0 s and 6.0 s, ECRH was turned off and the NBI power increased to 5.0 MW. Since it was anticipated that the impurity confinement time in this phase would be the longest, impurity was injected at 4.5 s, a 1.5 s before the end of the flattop. Due to the dominant ion heating, the ratio of T_e/T_i dropped to 0.8 and $(R/L_{T_i} \sim 2 \cdot R/L_{T_e})$ inside of $\rho_t = 0.4$.

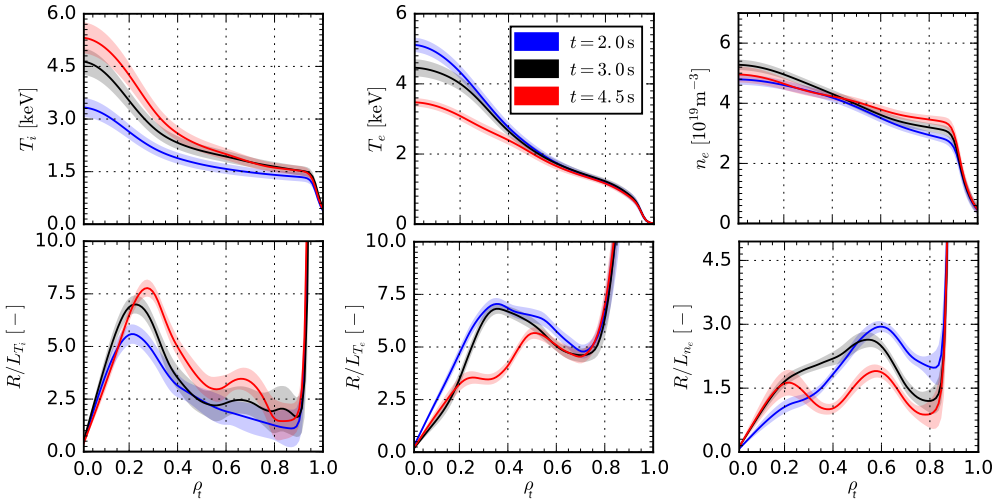

Figure 1: (upper row) Radial profiles of T_i, T_e, n_e and corresponding normalized scale lengths (lower row) for each heating phase in the ECRH/NBI scan.

Beam torque was fixed to 2 Nm in the entire discharge by applying a counter-current directed NBI to avoid a fast spinning of the plasma and a change in $E \times B$ shear during the NBI scan. The rotation was below 50 krad/s at midradius, which corresponds to a deuterium Mach number $M_D = 0.2$, causing negligible centrifugal asymmetry of Al ions and 20% asymmetry of W ions. Weak asymmetry is known to reduce the magnitude of a neoclassical impurity flux [2].

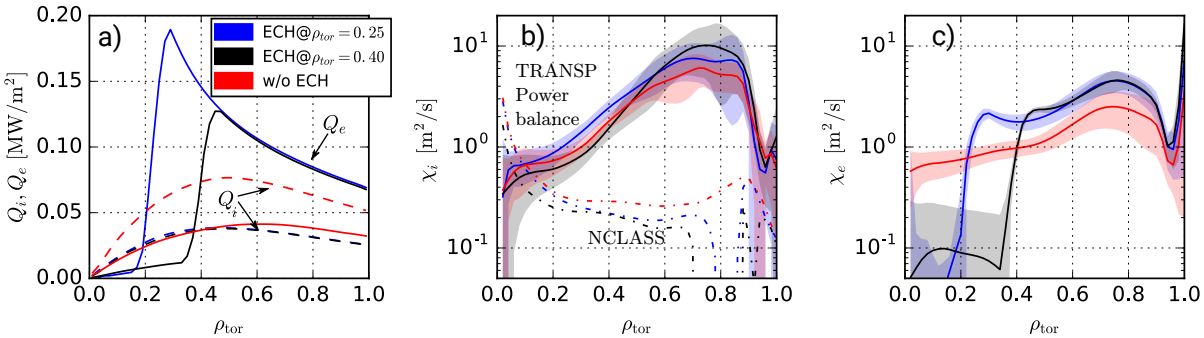

Figure 2: Example of (a) heat flux and (b,c) thermal diffusivities profiles obtained from a TRANSP power balance during the ECRH position scan.

ECRH Power and Position Scan

In this section, we compare results from a 3 point scan of ECRH deposition. The conditions studied were with ECRH at $\rho_t = 0.25$, $\rho_t = 0.4$ and NBI heating only. In these discharge, it is found that the electron heat flux increases by more than an order if magnitude in the ECH deposition region as shown in Fig. 2a.The low collisionality ($\nu_e^* = 0.04$), the electron-ion exchange heat flux Q_{ie} was below 15 kW/m^2. Ion heat diffusion in Fig. 2b has increased by a factor of 2 inside of $\rho_t = 0.5$ for central ECRH compared to off-axis and the NBI only case. Outside the ECH deposition region, χ_e also doubles compared to the non-ECH case as shown in Fig. 2c.

The impurity transport coefficients were evaluated by a direct comparison of the SXR emissivity with the solution of a diffusion-convection equation [1]. The conversion factor between impurity density and SXR radiation is calculated using the STRAHL code [6] and atomic data from ADAS database [7]. Profiles of D and V/D best matching the local SXR emissivity ob-

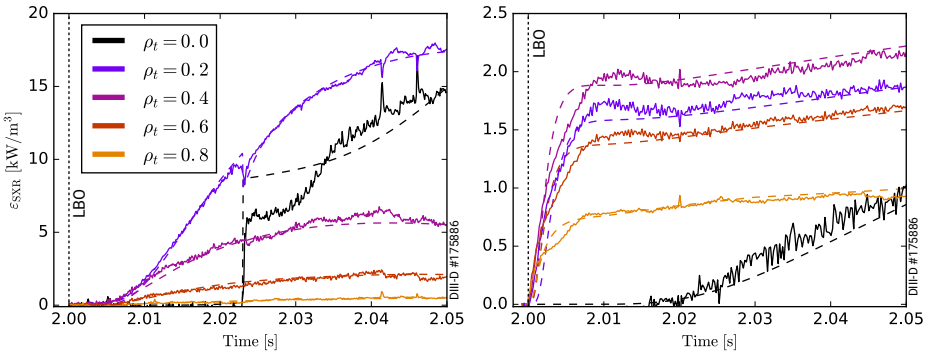

Figure 3: Background subtracted evolution of SXR emissivity after W (left) and Al (right) LBO injection with 3 MW ECRH at $\rho_t = 0.25$. The dashed line corresponds to the least square fit by a transport model used to determine transport coefficients.

tained from tomographic inversion [4] were identified via a least squares minimization procedure with the uncertainty quantified based on a Markov chain Monte Carlo (MCMC) method [5]. Due to the presence of ELMs in these discharges, only the rise phase of the SXR emissivity (prior to the first ELM) was analyzed. Evolution of local SXR emissivity after W and Al injection is illustrated in Fig. 3. Al ions travel quickly inwards and reach the ECRH heating position ($\rho_t = 0.25$) in about 10 ms, while the W emissivity is increasing for 50 ms after LBO injection. Emissivity on axis ($\rho_t = 0.0$) evolves much slower in both cases, indicating very low transport close to magnetic axis. Quantification of the transport coefficients is presented in Fig. 4 for Al and Fig. 5 for W. The inferred diffusion coefficient of Al is about 0.1 m^2/s in the core for all three cases considered. However outside of the ECRH heating position the diffusion coefficient increases, reaching levels that are 1-2 orders of magnitude higher than in the NBI-only case. Despite a large uncertainty in D profile, the value must be at least 30 m^2/s at midradius to explain the fast transport in Fig. 3b. The complementary set of D and V/D profiles for W impurity

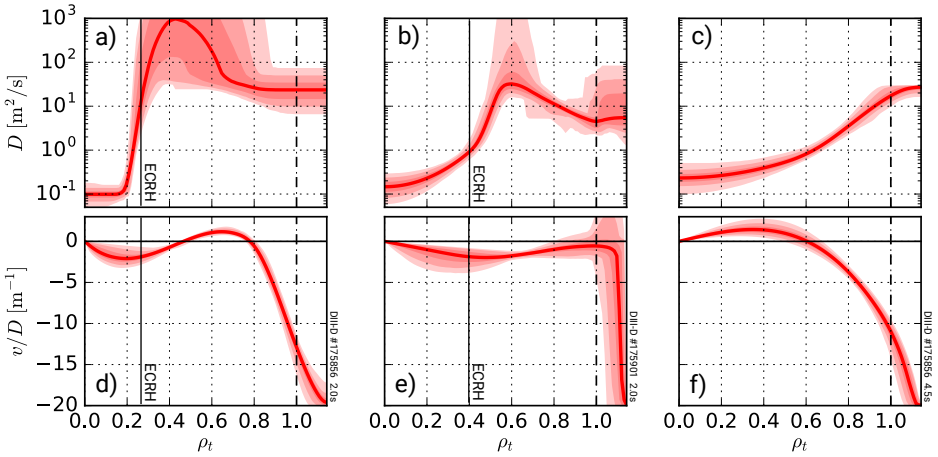

Figure 4: Diffusion coefficient D (*a-c*) and peaking factor V/D (*d-f*) of Al ions.

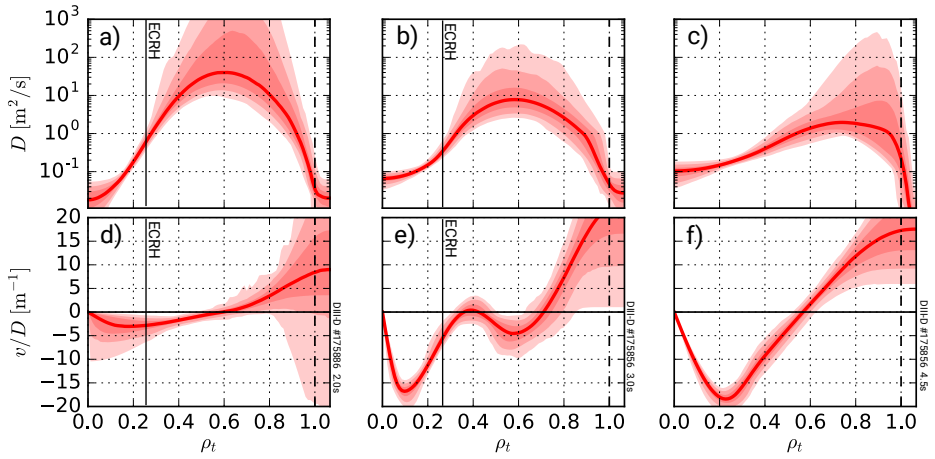

Figure 5: Profiles of D and V/D for W ions: (a,d) $P_{\mathrm{ECR}} = 2.9\,\mathrm{MW}$, $P_{\mathrm{NBI}} = 2\,\mathrm{MW}$, (b,e) $P_{\mathrm{ECR}} = 1.8\,\mathrm{MW}$, $P_{\mathrm{NBI}} = 3.4\,\mathrm{MW}$ and (c,f) $P_{\mathrm{NBI}} = 5\,\mathrm{MW}$

injection during ECRH/NBI power scan is displayed in Fig. 5. Diffusion inside of the heating position is also of the order of $0.1\,\mathrm{m}^2/\mathrm{s}$ for all three cases. Outside of the ECRH resonance, D significantly decreases with the reduction of ECRH power. Interestingly, the slow evolution of SXR signals in Fig. 3a appears to result from a narrow region of very low diffusion close to the edge of the plasma that was not observed in case of Al injections. The V/D coefficient describing a peaking of the stationary impurity density profile is decreasing from an almost negligible value and flat profile for maximal ECRH power to a strongly peaked profile with $-20\,\mathrm{m}^{-1}$ in the NBI only case.

Summary and Outlook

Compared to the previous study of R. Dux [1] on the ASDEX Upgrade tokamak, where an non-local enhancement of D by factor 3-5 to value $0.3\,\mathrm{m}^2/\mathrm{s}$ was reported with the application of ECRH, we have observed a very significant localized increase of diffusive flux outside of the heating radius to 10-30 m^2/s for Al ions and smaller and less localized, but still substantial increase for W ions to 5-10 m^2/s. The large difference in the evolution of W and Al density profiles appears to result from very different values of D at the plasma edge. Detailed comparisons of inferred transport coefficients with the neoclassical and gyrokinetic codes as well as investigation of turbulence changes using fluctuation diagnostics is part of the ongoing work.

Acknowledgment

This work was supported by U.S. Department of Energy award DE-SC0014264 and DIII-D cooperative agreement DE-FC02-04ER54698.

References

[1] Dux R. et al., OOCF **45**, 1815-1825 (2003).
[2] Odstrcil T. et al., PPCF **60.1** (2017).
[3] Hollmann, E. M., et al., RSI**82.11** (2011)
[4] Odstrcil T. et al. RSI **87.12** (2016)
[5] Goodman, J, Comm App Math Comp Sci 2010, 5.1: 65-80.
[6] R. Dux. STRAHL User Manual.IPP 10/30, (2014)
[7] Summers, H. P. (2004) The ADAS User Manual, version 2.6 http://www.adas.ac.uk